QCD material parameters at zero and non-zero chemical potential from the lattice

David Anthony Clarke[1,*], *Jishnu* Goswami[2], *Frithjof* Karsch[3], and *Peter* Petreczky[4]

[1]Department of Physics and Astronomy, University of Utah, Salt Lake City, Utah 84112, United States
[2]RIKEN Center for Computational Science, Kobe 650-0047, Japan
[3]Fakultät für Physik, Universität Bielefeld, D-33615 Bielefeld, Germany
[4]Physics Department, Brookhaven National Laboratory, Upton, New York 11973, USA

Abstract. Using an eighth-order Taylor expansion in baryon chemical potential, we recently obtained the (2+1)-flavor QCD equation of state (EoS) at non-zero conserved charge chemical potentials from the lattice. We focused on strangeness-neutral, isospin-symmetric QCD matter, which closely resembles the situation encountered in heavy-ion collision experiments. Using this EoS, we present here results on various QCD material parameters; in particular we compute the specific heat, speed of sound, and compressibility along appropriate lines of constant physics. We show that in the entire range relevant for the beam energy scan at RHIC, the specific heat, speed of sound, and compressibility show no indication for an approach to critical behavior that one would expect close to a possibly existing critical endpoint.

1 Introduction

A major goal of the experimental program on heavy-ion collisions (HIC) is to investigate transport and thermodynamic properties of strongly-interacting matter in the plane of temperature T and baryon chemical potential μ_B. Included among these properties are material parameters like the speed of sound, the compressibility, and the specific heat. The isentropic speed of sound c_s^2 is interesting, e.g., in the context of neutron stars since the relationship between the star masses and radii is influenced by how c_s^2 changes with baryon number density n_B [1]. The isothermal speed of sound c_T^2 is also interesting for HIC, as a new method to estimate c_T^2 in HIC has been recently suggested in Ref. [2]. Finally the isovolumetric specific heat C_V can be related to the temperature fluctuations in HIC [3].

It is of special interest to probe the μ_B-T plane for $\mu_B > 0$, where a hypothesized first-order line separating a hadronic gas phase and a quark-gluon plasma phase terminates in a critical endpoint (CEP). Material parameters provide useful information about the nature of the CEP. For example c_s^2 would drop to zero at a true phase transition, and at a second-order transition, C_V would show a singularity.

Some of these material parameters have been previously calculated on the lattice at $\mu_B = 0$ [4–6]. Here we present our ongoing calculations of these quantities at nonzero μ_B.

*e-mail: clarke.davida@gmail.com

2 Strategy of the calculation

We define $\hat{X} \equiv XT^{-k}$ with $k \in \mathbb{Z}$ chosen so that $\hat{X}$ is unitless. We expand the pressure $\hat{p}$ in terms of the conserved charge chemical potentials $\hat{\mu}_B, \hat{\mu}_Q, \hat{\mu}_S$ as

$$\hat{p} = \frac{1}{VT^3} \log \mathcal{Z}_{\mathrm{QCD}}(T, V, \hat{\mu}_B, \hat{\mu}_Q, \hat{\mu}_S) = \sum_{i,j,k=0}^{\infty} \frac{\chi_{ijk}^{BQS}}{i!j!k!} \hat{\mu}_B^i \hat{\mu}_Q^j \hat{\mu}_S^k, \tag{1}$$

where $\mathcal{Z}_{\mathrm{QCD}}$ is the QCD grand partition function, V is the spatial volume, and

$$\chi_{ijk}^{BQS} \equiv \chi_{ijk}^{BQS}(T) = \left. \frac{\partial \hat{p}}{\partial \hat{\mu}_B^i \partial \hat{\mu}_Q^j \partial \hat{\mu}_S^k} \right|_{\vec{\mu}=0} . \tag{2}$$

Other observables such as the entropy density $\hat{s}$ and net-charge densities $\hat{n}$ are derived from $\hat{p}$ using standard thermodynamic relations. To limit our analysis to the μ_B-T plane while focusing on the relevant physics of HIC, we impose constraints $n_S = 0$ and $n_Q/n_B = r$. In the following, partial derivatives are understood to be evaluated at fixed r and n_S. We focus on

$$c_s^2 = \left(\frac{\partial p}{\partial \epsilon}\right)_{s/n_B}, \quad c_T^2 = \left(\frac{\partial p}{\partial \epsilon}\right)_T, \quad \kappa_s = \frac{1}{n_B}\left(\frac{\partial n_B}{\partial p}\right)_{s/n_B}, \quad C_V = T\left(\frac{\partial s}{\partial T}\right)_{n_B}, \tag{3}$$

where ϵ is the energy density. In our previous work [7] we computed c_s^2 using lattice data for various s/n_B. To do this, we exploited the fact that

$$c_s^2 = \left(\frac{\partial p/\partial T}{\partial \epsilon/\partial T}\right)_{s/n_B} . \tag{4}$$

We then interpolated p and ϵ results simulated at various T and computed the derivative numerically. While this approach is straightforward, it is not ideal to use interpolations since the numerical derivatives, especially higher-order ones, are quite sensitive to the interpolation result. Since we estimate errors using a bootstrap procedure, this can lead to substantially different estimates for the derivatives in each bin and hence an artificially large error bar.

Now we address these large statistical uncertainties by utilizing analytic formulas for the material parameters in terms of cumulants, reducing the need to interpolate as much as possible. Besides yielding more controlled uncertainties in the lattice data, we found this approach increases numerical stability for our fixed s/n_B HRG results, allowing us to extend our calculations as low as $s/n_B = 10$ [8]. When possible, our analytic formulas are cross-checked against known thermodynamic relations; for instance we find our expressions for c_s and κ_s to formally satisify $\kappa_s^{-1} = c_s^2(\epsilon + p - \mu_Q n_Q - \mu_S n_S)$.

3 Computational setup

We use high-statistics data sets for (2 + 1)-flavor QCD with degenerate light quark masses $m_u = m_d \equiv m_l$ and a strange quark mass m_s tuned so that $m_s/m_l = 27$. These are the same data sets as in Ref. [9, 10]. We employed a HISQ action generated using `SIMULATeQCD` [11, 12]. Temperatures above 180 MeV use data [9] with slightly heavier[1] light quarks, $m_s/m_l = 20$. In all cases results have been obtained on lattices with aspect ratio $N_\sigma/N_\tau = 4$. In these proceedings, we present calculations only for the isospin-symmetric case $r = 0.5$. While $r =$

[1] This is known to have a negligible effect on the results [13].

0.4 is a more physically accurate choice, choosing $r = 0.5$ has the advantage of forcing $\hat{\mu}_Q = 0$, simplifying some of the formulas. Moreover the quantitative differences between $r = 0.4$ and $r = 0.5$ EoS are generally mild [14] and are hence expected to have little impact on these parameters[2]. We are often interested in the behavior of observables near the pseudocritical temperature $T_{\rm pc}$. When indicated on figures, we take $T_{\rm pc} = 156.5(1.5)$ MeV from Ref. [15]. Lines of constant s/n_B and n_B/n_0, with nuclear matter density $n_0 = 0.16/\text{fm}^3$, are taken from Ref. [7]. The `AnalysisToolbox` [16] is used for HRG calculations, spline fits, and bootstrapping. For the HRG model, we use the QMHRG2020 list of hadron resonances [17].

4 Results

In Fig. 1 we show preliminary results for c_s^2, c_T^2, κ_s, and C_V. Not all uncertainty has been included, hence error bands are mildly underestimated. Starting with isentropic observables, we note that because n_B leads at $O(\mu_B)$ while s leads with a constant, the limit $\mu_B \to \infty$ corresponds to $s/n_B \to 0$. Hence the left-hand plots show an at most mild dependence on μ_B in the surveyed range. We see no indication of c_s^2 going to zero within this range and hence no critical signature. As has been seen already with $\mu_B = 0$ calculations, c_s^2 overlaps with the estimate from Ref. [18], and both isentropic observables agree with our previous computation in Ref. [7]. Turning to c_T^2, our preliminary results are similar to the preliminary results of Ref. [8]. Finally our results for C_V at $\mu_B = 0$ agree with previous HotQCD results [6]. For all observables we see good agreement between lattice data and HRG below $T_{\rm pc}$.

5 Summary and outlook

We presented the status of our ongoing calculation of various QCD material parameters. The computation of the thermal expansion coefficient and isobaric heat capacity are in progress, which besides being interesting in their own right, will enable a few more analytic cross-checks between the parameters. For all our projects involving the QCD EoS, it will be useful to eventually have continuum extrapolations for 6$^{\text{th}}$- and 8$^{\text{th}}$-order cumulants, but this is a much more long-term goal.

Acknowledgements–DAC was supported by the National Science Foundation under Grants PHY20-13064 and PHY23-10571.

References

[1] F. Özel, P. Freire, Ann. Rev. Astron. Astrophys. **54**, 401 (2016), `1603.02698`

[2] A. Sorensen, D. Oliinychenko, V. Koch, L. McLerran, Phys. Rev. Lett. **127**, 042303 (2021), `2103.07365`

[3] E.V. Shuryak, Phys. Lett. B **423**, 9 (1998), `hep-ph/9704456`

[4] R.V. Gavai, S. Gupta, S. Mukherjee, Phys. Rev. D **71**, 074013 (2005), `hep-lat/0412036`

[5] S. Borsanyi, Z. Fodor, C. Hoelbling, S.D. Katz, S. Krieg, K.K. Szabo, Phys. Lett. B **730**, 99 (2014), `1309.5258`

[6] A. Bazavov et al. (HotQCD), Phys. Rev. D **90**, 094503 (2014), `1407.6387`

[7] D. Bollweg, D.A. Clarke, J. Goswami, O. Kaczmarek, F. Karsch, S. Mukherjee, P. Petreczky, C. Schmidt, S. Sharma (HotQCD), Phys. Rev. D **108**, 014510 (2023), `2212.09043`

[2] Indeed, this is what we found for the sound speeds [8].

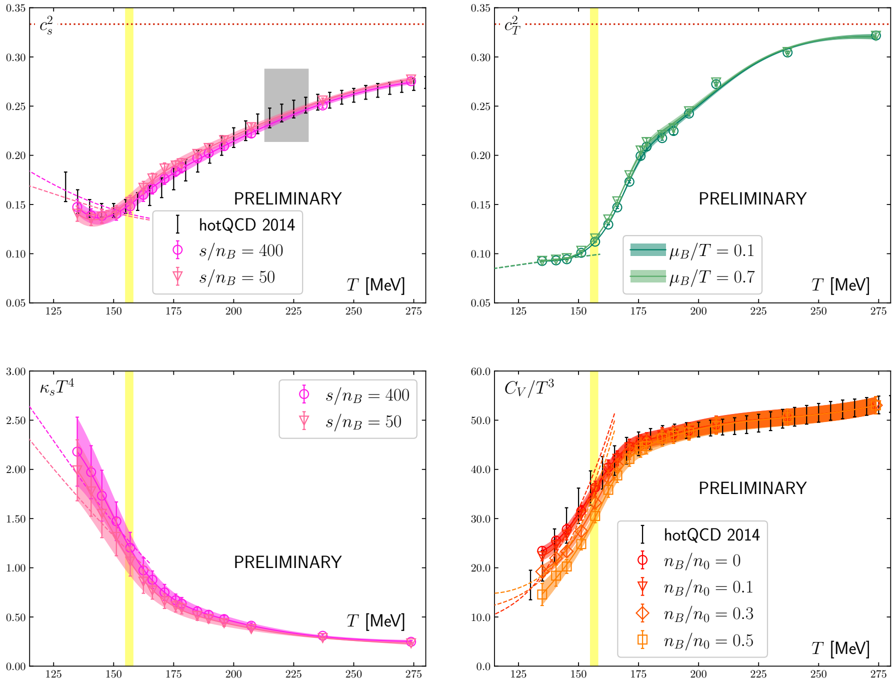

Figure 1. Material parameters at $r = 0.5$. The bands are a spline fit to the data and errors. The yellow band shows $T_{\rm pc}$. The dashed lines show the HRG result. For the sound speeds, the red, dotted line indicates the conformal limit. *Top left*: Isentropic speed of sound calculated using eqs. (C3), (C4), and (C5) of Ref. [7]. The grey box indicates c_s^2 extracted from hydrodynamic simulations using experimental data [18]. *Top right*: Isothermal speed of sound. *Bottom left*: Isentropic compressibility. *Bottom right*: Isovolumetric heat capacity. The hotQCD data, taken from Ref. [6], were computed at $\mu_B = 0$.

[8] D.A. Clarke, PoS **LATTICE2022**, 147 (2023), `2212.10009`

[9] A. Bazavov et al., Phys. Rev. D **95**, 054504 (2017), `1701.04325`

[10] D. Bollweg, J. Goswami, O. Kaczmarek, F. Karsch, S. Mukherjee, P. Petreczky, C. Schmidt, P. Scior (HotQCD), Phys. Rev. D **105**, 074511 (2022), `2202.09184`

[11] D. Bollweg, L. Altenkort, D.A. Clarke, O. Kaczmarek, L. Mazur, C. Schmidt, P. Scior, H.T. Shu, PoS **LATTICE2021**, 196 (2022), `2111.10354`

[12] L. Mazur et al. (HotQCD) (2023), `2306.01098`

[13] A. Bazavov et al. (HotQCD), Phys. Rev. D **85**, 054503 (2012), `1111.1710`

[14] J. Goswami (HotQCD), PoS **LATTICE2022**, 149 (2023), `2212.10016`

[15] A. Bazavov et al. (HotQCD), Phys. Lett. B **795**, 15 (2019), `1812.08235`

[16] L. Altenkort, D.A. Clarke, J. Goswami, H. Sandmeyer, PoS **LATTICE2023**, 136 (2023), `2308.06652`

[17] D. Bollweg, J. Goswami, O. Kaczmarek, F. Karsch, S. Mukherjee, P. Petreczky, C. Schmidt, P. Scior (HotQCD), Phys. Rev. D **104** (2021), `2107.10011`

[18] F.G. Gardim, G. Giacalone, M. Luzum, J.Y. Ollitrault, Nature Phys. **16**, 615 (2020), `1908.09728`